Eur. Phys. J. A **19**, 237–246 (2004)
DOI 10.1140/epja/i2003-10123-2

THE EUROPEAN PHYSICAL JOURNAL A

Centrality dependence of particle production at RHIC and the combinational approach

Bhaskar De[a] and S. Bhattacharyya[b]

Physics and Applied Mathematics Unit (PAMU), Indian Statistical Institute, Kolkata, 700108, India

Received: 2 April 2003 / Revised version: 29 July 2003 /
Published online: 23 December 2003 –
Communicated by A. Molinari

Abstract. The newly proposed combinational approach, called the grand combination of models (GCM), as will be described in detail in the text, is still under our careful scrutiny. By applying it, we have attempted to analyze here the characteristics of both the transverse momentum (p_{T})-, and centrality dependence of the production of the main varieties of the secondaries measured in AuAu collisions at BNL-RHIC at both $\sqrt{s_{NN}} = 130$ GeV and $\sqrt{s_{NN}} = 200$ GeV by PHENIX Collaboration. Besides, with the help of it, we have also investigated the nature of the centrality dependence of the average transverse momenta of the various major categories of particles in AuAu collisions at RHIC. The model seems to survive quite smoothly the acid tests of the latest PHENIX data, as it accommodates data modestly well on these twin aspects. The study reveals a kind of universality of nature of the hadronic secondaries and also of the basic particle and nuclear interactions at high energies. However, in the end, we precisely point out both the strengths and limitations of the specific model under consideration here.

PACS. 13.60.Hb Total and inclusive cross-sections (including deep-inelastic processes) – 25.75.-q Relativistic heavy-ion collisions

1 Introduction

In the recent past the PHENIX Collaboration conducted exhaustive measurements of the particle yields in AuAu collisions at RHIC-BNL at very high ranges of transverse-momentum values and also at various centralities of the collisions. The data sets on both identified centrality-dependent charged-hadron spectra *vs.* transverse momenta and also on the average-transverse-momentum values ($\langle p_{\mathrm{T}} \rangle$) of the various secondaries *vs.* the centralities of the collisions [1,2] were indicated by the graphical plots shown in various figures presented here. These measurements were mainly aimed at checking some predictions from the Standard Model (SM) on i) the suppression of particle yields at large transverse momenta and ii) the dependence of the degree of suppression on the centrality of the collision. In the framework of the standard model, all the secondary particles are produced by jets. These jets are likely to suffer significant energy loss via "gluon" radiation, while passing through the hot dense medium arising out of the anticipated QGP formation. So, according to this view, the particle yield at large p_{T} should be suppressed to a considerable degree. Secondly, since the amount of energy loss is a function of the density and the path length through such a projected QGP media, the suppression effect is predicted to be dependent also on the centrality of the collision [3]. All the theoretical postulates and predictions serve as the background for such intense attempts at measurements.

But in our approach we would maintain a degree of neutrality to such standard theoretical views and would concern ourselves mainly with the results of measurements with the ulterior motive of checking and testing an alternative approach, called here the combinational approach or the grand combination of models (GCM) which will be utilized here to explain the sets of data on i) identified charged-hadron spectra *vs.* p_{T} values and ii) the values of the average transverse momentum, denoted by $\langle p_{\mathrm{T}} \rangle$, *vs.* the different centrality ranges of the AuAu reaction in particular.

The work is organized as follows: In sect. 2 we offer an outline of the GCM to be made use of in the present study. Section 3 contains and depicts the concrete results obtained on the basis of this model in the tabular forms and the graphical plots. The last section presents, as usual, the summary and final comments.

[a] e-mail: bhaskar_r@isical.ac.in
[b] e-mail: bsubrata@isical.ac.in

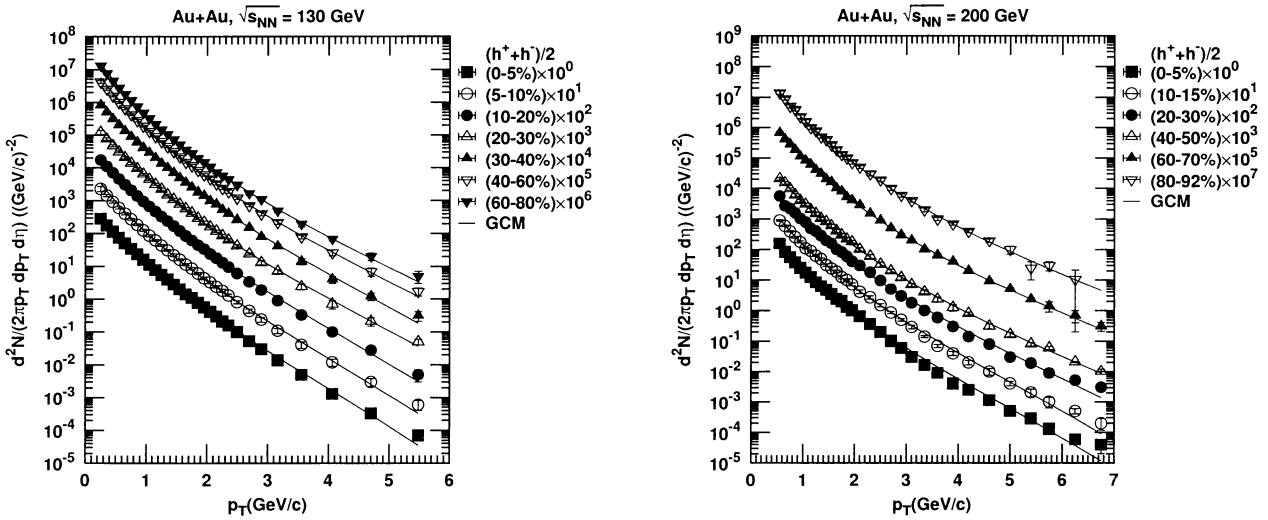

(a) (b)

Fig. 1. Plots of invariant spectra of secondary charged hadrons produced in AuAu collisions at two different RHIC energies for various centrality bins. The experimental data points are taken from ref. [4] for $\sqrt{s_{NN}} = 130$ GeV and from ref. [3] for $\sqrt{s_{NN}} = 200$ GeV, respectively. The solid curves provide the GCM-based fits.

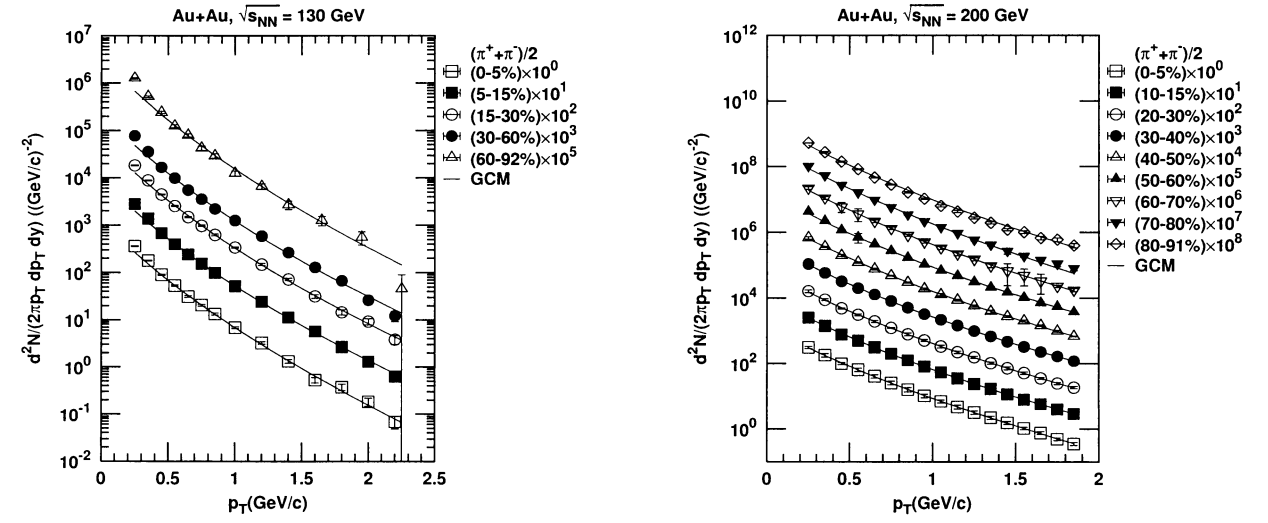

(a) (b)

Fig. 2. Nature of invariant spectra of secondary charged pions produced in AuAu collisions at two different RHIC energies at different centralities as a function of $p_{\rm T}$. The experimental data points at $\sqrt{s_{NN}} = 130$ GeV are taken from ref. [5], while those for $\sqrt{s_{NN}} = 200$ GeV are from ref. [1]. The solid curves are drawn on the basis of eq. (6).

2 The model: a sketch

Following the suggestion of Faessler [6] and the work of Peitzmann [7] and also of Schmidt and Schukraft [8], we propose here a generalized empirical relationship between the inclusive cross-sections for any variety of the secondaries (Q), such as hadrons, pions, kaons or proton/antiprotpons, produced in nucleon (N)-nucleon (N) collision and that for nucleus (A)-nucleus (B) collision as given below:

$$E\frac{{\rm d}^3\sigma}{{\rm d}p^3}(AB \to QX) \sim (AB)^{\phi(y,p_{\rm T})} E\frac{{\rm d}^3\sigma}{{\rm d}p^3}(PP \to QX)\,, \tag{1}$$

where $\phi(y, p_{\rm T})$ could be expressed in the factorization form, $\phi(y, p_{\rm T}) = f(y)g(p_{\rm T})$, and the product, AB on the right-hand side of the above equation is the product of mass numbers of the two nuclei participating in

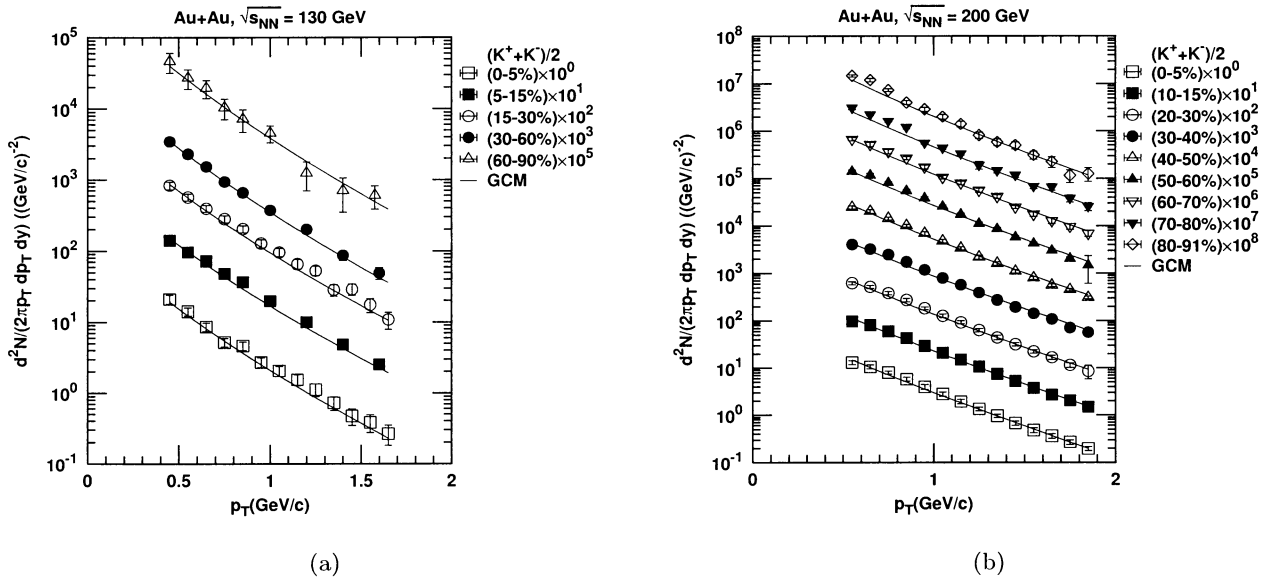

(a) (b)

Fig. 3. Transverse-momentum spectra for the production of secondary charged kaons in AuAu collisions at two different RHIC energies at different centralities. The various experimental data points at $\sqrt{s_{NN}} = 130$ GeV are taken from ref. [5], while those for $\sqrt{s_{NN}} = 200$ GeV are from ref. [1]. The present model (GCM)-based fits are depicted by the solid curvilinear lines.

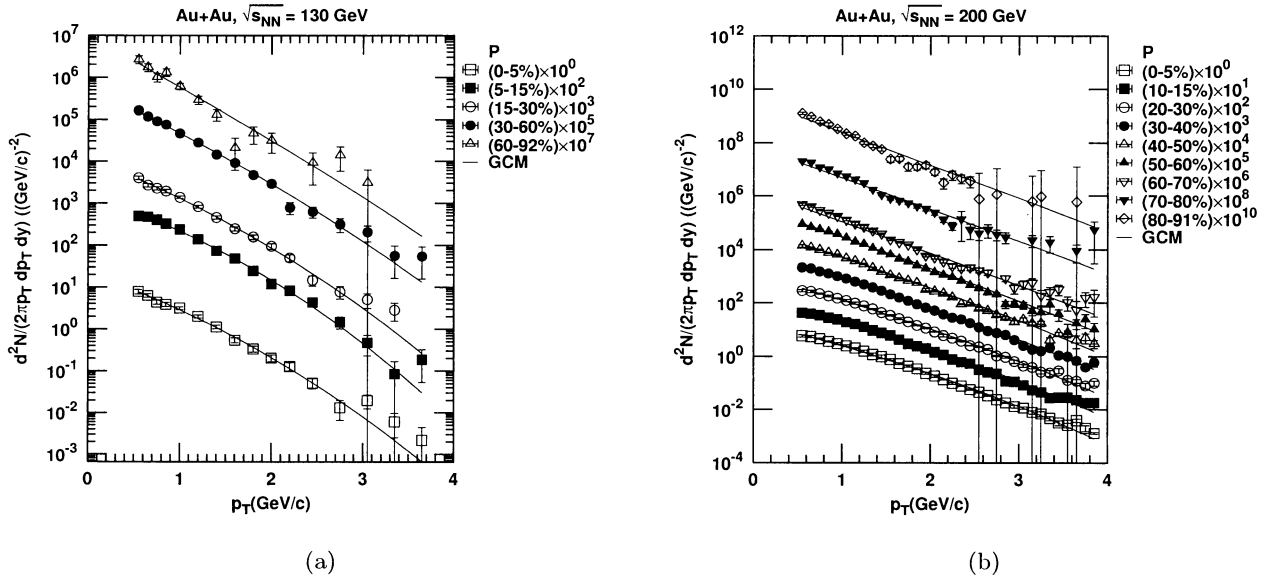

(a) (b)

Fig. 4. Plots of invariant spectra for the production of secondary protons in AuAu collisions at two different RHIC energies at different centralities. The various experimental data points at $\sqrt{s_{NN}} = 130$ GeV are taken from ref. [5], while those for $\sqrt{s_{NN}} = 200$ GeV are from ref. [1]. The GCM-based fits are depicted by the solid curves.

the collisions at high energies, of which one will be the projectile and the other one the target, respectively.

While investigating the specific nature of the dependence of the two variables (y and p_{T}), either of them is assumed to remain averaged or with definite values. Speaking in clearer terms, if and when the p_{T}-dependence is studied by the experimental group, the rapidity factor is integrated over certain limits and is absorbed in the normalization factor. So, the formula turns into

$$E\frac{\mathrm{d}^3\sigma}{\mathrm{d}p^3}(AB \to QX) \sim (AB)^{g(p_{\mathrm{T}})} E\frac{\mathrm{d}^3\sigma}{\mathrm{d}p^3}(PP \to QX)\,. \quad (2)$$

The main bulk of work, thus, converges to the making of an appropriate choice of form for $g(p_{\mathrm{T}})$. And the necessary choices are to be made on the basis of certain premises and physical considerations which do not violate the canons of high-energy particle interactions.

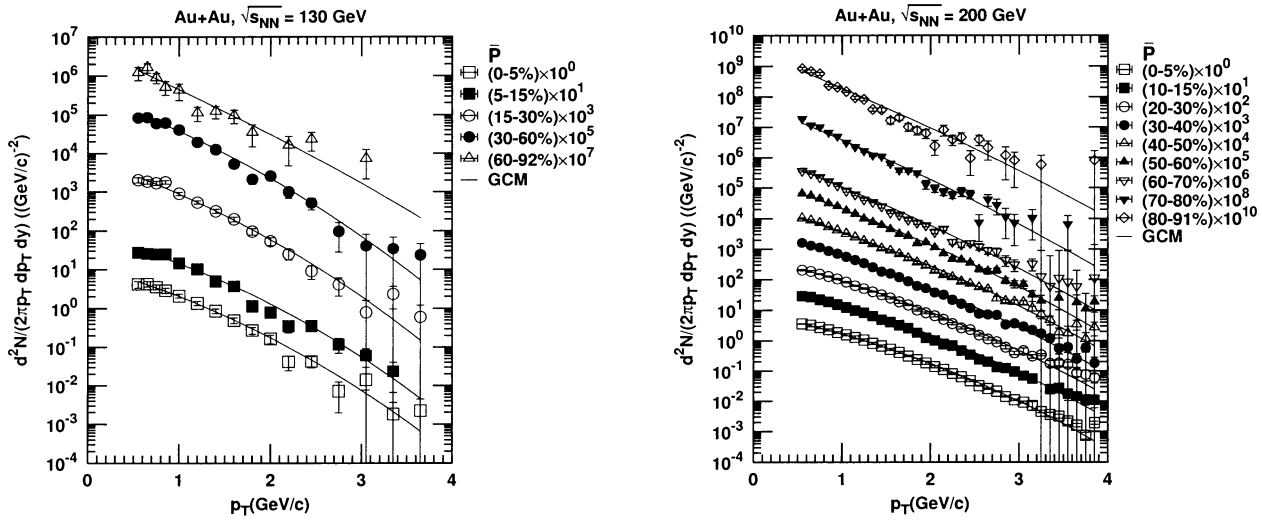

(a) (b)

Fig. 5. Nature of invariant spectra of secondary antiprotons produced in AuAu collisions at two different RHIC energies at different centralities as a function of $p_{\rm T}$. The experimental data points at $\sqrt{s_{NN}} = 130$ GeV are taken from ref. [5], while those for $\sqrt{s_{NN}} = 200$ GeV are from ref. [1]. The solid curves are drawn on the basis of eq. (6).

The expression for the inclusive cross-section of Q in proton-proton scattering at high energies occurring in eq. (2) could be chosen in the form suggested first by Hagedorn [9]:

$$E\frac{\mathrm{d}^3\sigma}{\mathrm{d}p^3}(PP \to QX) = C_1\left(1+\frac{p_{\rm T}}{p_0}\right)^{-n}, \qquad (3)$$

where C_1 is the normalization constant, and p_0, n are interaction-dependent chosen phenomenological parameters for which the values are to be obtained by the method of fitting the spectra in the PP interaction.

The final working formula for the nucleus-nucleus collisions is proposed here in the form given below:

$$E\frac{\mathrm{d}^3\sigma}{\mathrm{d}p^3}(AB \to QX) \propto (AB)^{(\epsilon+\alpha p_{\rm T}-\beta p_{\rm T}^2)} E\frac{\mathrm{d}^3\sigma}{\mathrm{d}p^3}(PP \to QX)$$
$$\propto (AB)^{(\epsilon+\alpha p_{\rm T}-\beta p_{\rm T}^2)}\left(1+\frac{p_{\rm T}}{p_0}\right)^{-n}, \quad (4)$$

with $g(p_{\rm T}) = (\epsilon + \alpha p_{\rm T} - \beta p_{\rm T}^2)$, where this suggestion of quadratic parametrization for $g(p_{\rm T})$ is exclusively made by us and is called hereafter De-Bhattacharyya parametrization (DBP). In the above expression ϵ, α and β are constants for a specific pair of projectile and target.

Earlier experimental works [10–12] showed that $g(p_{\rm T})$ is less than unity in the $p_{\rm T}$ domain, $p_{\rm T} < 1.5$ GeV/c. Besides, it was also observed that the parameter ϵ, which gives the value of $g(p_{\rm T})$ at $p_{\rm T} = 0$, is also less than unity and this value differs from collision to collision. The other two parameters α and β essentially determine the nature of the curvature of $g(p_{\rm T})$. However, in the present context, a precise determination of ϵ is not possible for the following understated reasons:

i) To make our point let us recast the expression for (4) in the form given below:

$$E\frac{\mathrm{d}^3\sigma}{\mathrm{d}p^3}(AB \to QX) \approx C_2(AB)^{\epsilon}(AB)^{(\alpha p_{\rm T}-\beta p_{\rm T}^2)}\left(1+\frac{p_{\rm T}}{p_0}\right)^{-n}, \qquad (5)$$

where C_2 is the normalization term which has a dependence either on the rapidity or on the rapidity density of the Q and which also absorbs the previous constant term, C_1 as well.

Quite obviously, we have adopted here the method of fitting. Now, in eq. (5) one finds that there are two constant terms C_2 and ϵ which are neither the coefficients nor the exponent terms of any function of the variable, $p_{\rm T}$. And as ϵ is a constant for a specific collision at a specific energy, the product of the two terms C_2 and $(AB)^{\epsilon}$ appears as just a new constant. And, it will just not be possible to obtain fit values simultaneously for two constants of the above types by the method of fitting.

ii) From eq. (2) the nature of $g(p_{\rm T})$ can easily be determined by calculating the ratio of the logarithm of the ratios of the nuclear-to-PP collision and the logarithm of the product AB. Thus, one can measure ϵ from the intercept of $g(p_{\rm T})$ along the y-axis as soon as one gets the values of $E\frac{\mathrm{d}^3\sigma}{\mathrm{d}p^3}$ for any specific secondary production in both AB collision and PP collision at the same c.m. energy. In the present study we have tried to consider the AuAu collision system in various centrality bins at two different c.m. energies. In order to do so, we have to consider the data on normalized versions of $E\frac{\mathrm{d}^3\sigma}{\mathrm{d}p^3}$ for any secondary particle produced in this collision system for which no clear $E\frac{\mathrm{d}^3\sigma}{\mathrm{d}p^3}$ data is available to us. Furthermore, from these normalized versions we can/could not extract the appropriate values of $E\frac{\mathrm{d}^3\sigma}{\mathrm{d}p^3}$ as the normalization terms, total

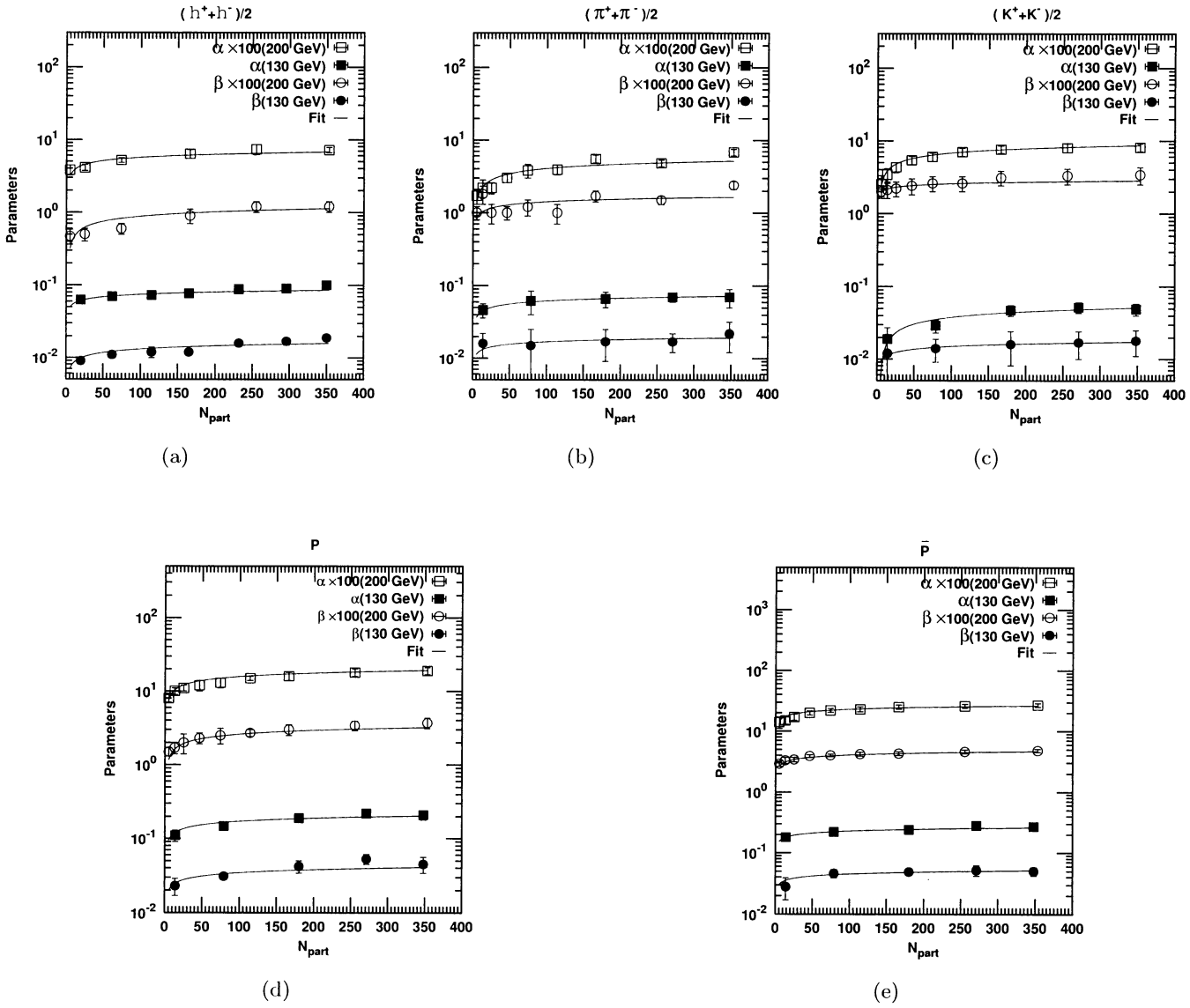

Fig. 6. Plots of α (in (c/GeV)) and β (in $(c/\mathrm{GeV})^2$) as a function of the number of participant nucleons, N_{part}. The different data type points for various secondaries are taken from table 2–table 11 below. Various solid curves are drawn on the basis of eq. (9) and denoted as "Fit" in the panels.

inclusive cross-sections (σ_{in}) etc., for this collision system at all centrality bins cannot always be readily obtained. Besides, it will also not be possible to get readily the data on inclusive spectra for PP collisions at all c.m.energies.

In order to sidetrack these difficulties and also to build up an escape route, we have concentrated here almost wholly on the values of α and β for various collision systems and the resultant effects of C_2 and ϵ have been absorbed into a single constant term C_3. Hence, the final expression becomes

$$E\frac{\mathrm{d}^3\sigma}{\mathrm{d}p^3}(AB \to QX) \approx C_3(AB)^{(\alpha p_{\mathrm{T}} - \beta p_{\mathrm{T}}^2)} \left(1 + \frac{p_{\mathrm{T}}}{p_0}\right)^{-n} \tag{6}$$

with $C_3 = C_2(AB)^{\epsilon}$.

The exponent factor term $\alpha p_{\mathrm{T}} - \beta p_{\mathrm{T}}^2$ obviously represents here $[g(p_{\mathrm{T}}) - \epsilon]$ instead of $g(p_{\mathrm{T}})$ alone. Expression (6) given above is the physical embodiment of what we have termed to be the grand combination of models (GCM) that has been utilized here. The results of PP scattering are obtained in the above on the basis of eq. (3) provided by Hagedorn's model (HM); and the route for converting the results of NN to NA or AB collisions is built up by the Peitzmann's approach (PA) represented by expression (2). The further input is the De-Bhattacharyya parametrization for the nature of the exponent. Thus, the GCM is the combination of HM, PA and the DBP, all of which are used here.

Moreover the choice of this form of parametrization for the power of the exponent in eq. (4) is not altogether a coincidence. In dealing with the EMC effect in the lepton-nucleus collisions, one of the authors here (SB) [13] made use of a polynomial form of A-dependence with a

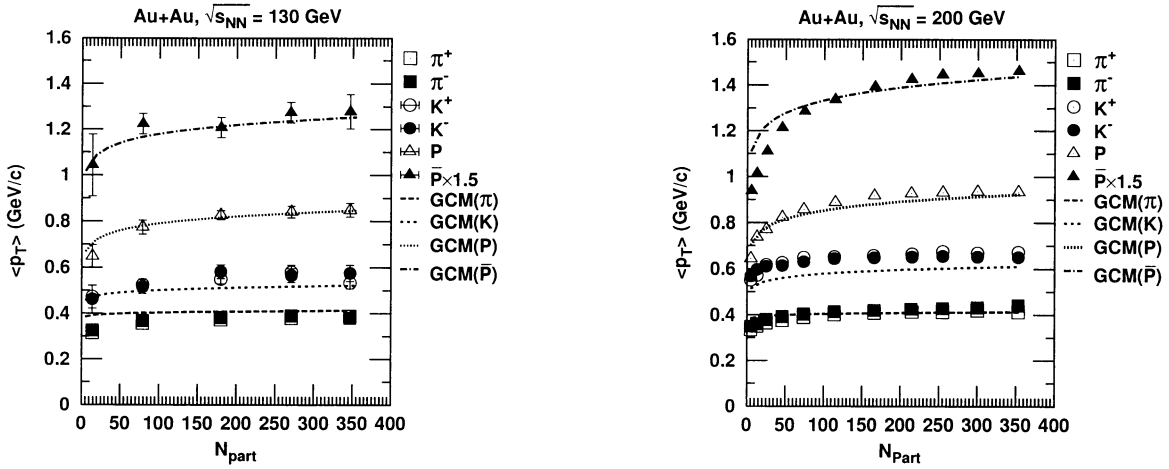

(a) (b)

Fig. 7. Nature of average transverse momenta ($\langle p_{\rm T}\rangle$) for various secondaries produced in AuAu collisions at two different energies as a function of $N_{\rm part}$. The data type points are the extracted results obtained by RHIC experimental groups [1]. The GCM-based results are shown by various dashed and dotted curves.

variable x which is a variant of $x_{\rm F}$ (the Feynman scaling variable). This gives us a clue to make a similar choice for both $g(p_{\rm T})$ and $f(y)$ variable(s) in each case separately. In recent times, De-Bhattacharyya parametrization has been extensively applied to interpret the measured data on the various aspects [14–17] of the particle-nucleus and nucleus-nucleus interactions at high energies. In the recent past Hwa *et al.* [18] also have made use of this sort of relationship in a somewhat different context. The underlying physics implications of this parametrization stem mainly from expression (4) which could be identified as a clear mechanism for switch-over of the results obtained for nucleon-nucleon (PP) collision to those for nucleus-nucleus interactions at high energies in a direct and straightforward manner. The polynomial exponent of the product term on AB takes care of the totality of nuclear effects.

For the sake of clarity and confirmation, let us further emphasize a point here very categorically. It is to be noted that this model (GCM) containing all the eqs. (4), (5) and (6) was described in some detail earlier and was made use of in analyzing extensive sets of data in the previous publications [14,15,17] by the same authors. And in verifying the validity of this model further, the purpose here is to apply the same model to some other problematical aspects of data which we would dwell upon in the subsequent sections. Before taking them up, let us state a point. In some previous works [15–17] we tried to provide some sort of physical interpretations for some of the parameters used in the present work. But, those explanations were only of suggestive nature. Besides, obviously, they are not complete and sufficient, for which we have chosen not to reiterate them here once more.

Table 1. Values of a, b, a' and b' used in eq. (7) and in eq. (8) to obtain p_0 and n for various secondaries.

Secondary type	a	b	a'	b'
h,π	1.5	79.4	6.5	127
K	1.6	103	3.6	161
P	7	602	5	644
$\bar{P}$	7	478	13	527

3 Presentation of the results

Obviously the GCM is the model of our choice here. The inclusive spectra for the production of the main varieties of various secondaries produced in AuAu collisions at RHIC at both $\sqrt{s_{NN}} = 130$ GeV and $\sqrt{s_{NN}} = 200$ GeV and also at various centrality values have been worked out here phenomenologically and shown in several diagrams. The values of p_0 and n, occurring in eq. (3), which are essentially the contribution of PP collisions to the nucleus-nucleus collisions for the same secondaries produced at the same c.m. energies per nucleon, have been introduced by the following relationships:

$$p_0(\sqrt{s}) = a + \frac{b}{\sqrt{\frac{s_{NN}}{\rm GeV^2}}\ln\left(\sqrt{\frac{s_{NN}}{\rm GeV^2}}\right)}\,, \tag{7}$$

$$n(\sqrt{s}) = a' + \frac{b'}{\ln^2\left(\sqrt{\frac{s_{NN}}{\rm GeV^2}}\right)}\,, \tag{8}$$

These are products of just empirical analyses made earlier and reported in some of our previous works [14, 15]. The actually used values of the arbitrary parameters, a, b, a' and b' for various secondary particles are given in table 1.

Table 2. Parameter values for charged-hadrons (averaged) production in AuAu collision at $\sqrt{s_{NN}} = 130$ GeV.

Centrality	C_3	α (c/GeV)	β (c/GeV)^2	χ^2/n.d.f.
0–15%	1708 ± 42	0.10 ± 0.01	0.019 ± 0.002	1.127
5–10%	1487 ± 39	0.09 ± 0.01	0.017 ± 0.002	1.281
10–20%	1161 ± 31	0.088 ± 0.004	0.016 ± 0.001	1.401
20–30%	831 ± 21	0.077 ± 0.003	0.012 ± 0.001	1.425
30–40%	561 ± 15	0.073 ± 0.003	0.012 ± 0.002	1.590
40–60%	262 ± 5	0.070 ± 0.002	0.011 ± 0.001	0.714
60–80%	69 ± 2	0.063 ± 0.003	0.009 ± 0.001	0.214

Table 3. Parameter values for the production of charged hadrons (averaged) in AuAu collision at $\sqrt{s_{NN}} = 200$ GeV.

Centrality	C_3	α (c/GeV)	β (c/GeV)^2	χ^2/n.d.f.
0–5%	3015 ± 189	0.072 ± 0.006	0.012 ± 0.002	1.281
10–15%	1962 ± 120	0.0741 ± 0.006	0.012 ± 0.002	1.191
20–30%	1230 ± 111	0.064 ± 0.009	0.009 ± 0.002	1.847
40–50%	547 ± 32	0.052 ± 0.004	0.006 ± 0.001	0.943
60–70%	171 ± 8	0.041 ± 0.004	0.005 ± 0.001	0.403
80–91%	262 ± 5	0.070 ± 0.002	0.011 ± 0.001	0.521

Table 4. Parameter values for charged pions (averaged) produced in AuAu collision at $\sqrt{s_{NN}} = 130$ GeV.

Centrality	C_3	α (c/GeV)	β (c/GeV)^2	χ^2/n.d.f.
0–5%	1243 ± 113	0.07 ± 0.02	0.022 ± 0.010	0.948
5–15%	922 ± 44	0.07 ± 0.01	0.017 ± 0.005	0.399
15–30%	602 ± 47	0.066 ± 0.016	0.017 ± 0.008	1.077
30–60%	230 ± 24	0.062 ± 0.022	0.015 ± 0.010	1.774
60–90%	33 ± 10	0.046 ± 0.010	0.016 ± 0.006	1.859

The obtained values of the average yields of hadrons at various centralities have been depicted in fig. 1. The left panel is for $\sqrt{s_{NN}} = 130$ GeV and the right panel is for $\sqrt{s_{NN}} = 200$ GeV. Figure 2 describes pion production on a charge-neutral and average basis at both the energies. Similar is the case with kaons in fig. 3. The diagrams in fig. 4 reproduce data on proton production in AuAu collisions at the two RHIC energies. The solid curves in fig. 5 display the theoretical yields of antiprotons in AuAu reaction at various values of the centrality of the collision against measured data. The values of the parameters α and β have been initially chosen with the singular motivation of obtaining satisfactory fits to the data, though finally even this arbitrariness has led to some revelation of the specific nature of α and β as are shown in the plots of fig. 6 for the various secondaries in several panels.

The values of α and β to be used in obtaining our model-based results are shown in different tables (table 2–table 11). The extreme left columns in all of them contain information about the centrality of the reaction and the extreme right ones offer the χ^2/n.d.f. values. Even for the cases of proton and antiproton production, wherein the data suffer a high degree of uncertainty, the χ^2/n.d.f. values are modestly satisfactory. The systematic trends of the used values of α and β depict a harmony of their nature which have been hinted by table 12 and table 13, respectively and represented by the sets of diagrams in fig. 6. The solid lines in fig. 6 provide the phenomenological fits which can be expressed by a common relationship of the form given below:

$$\alpha(N_{\rm part}), \beta(N_{\rm part}) = R + S \ln (N_{\rm part}) \,. \tag{9}$$

The different values of R and S for various secondaries are given in table 12 and table 13.

A comment is in order here in a pre-emptive manner. The values of α and β shown in our previous work [14] even on AuAu collision could be and are little different from those depicted here for two reasons: i) The $p_{\rm T}$ range of the detected secondaries in the previous work was limited mostly in the region from 0.8 GeV/c to 3 GeV/c, whereas in the present case both the full low-$p_{\rm T}$ and a larger domain of high-$p_{\rm T}$ range for the secondaries (mainly charged hadrons) has been covered. ii) Secondly, in the former study [14] the minimum bias event was studied in the main. On the contrary, the present study has very much been centrality-specific and the data for the various centrality values of the AuAu collision have been served within a phenomenological framework.

The average-transverse-momenta values for the different categories of particles have, however, been worked out on the basis of the following expression:

$$\langle p_{\rm T} \rangle = \frac{\int_0^\infty p_{\rm T} \frac{{\rm d}N}{p_{\rm T} {\rm d}p_{\rm T}} {\rm d}p_{\rm T}^2}{\int_0^\infty \frac{{\rm d}N}{p_{\rm T} {\rm d}p_{\rm T}} {\rm d}p_{\rm T}^2} \,. \tag{10}$$

The values of α and β to be introduced for $\langle p_{\rm T} \rangle$ values are used in both energy-specific and particle-specific

Table 5. Parameter values for charged pions (averaged) produced in AuAu collision at $\sqrt{s_{NN}} = 200$ GeV.

Centrality	C_3	α (c/GeV)	β $(c/\mathrm{GeV})^2$	χ^2/n.d.f.
0–5%	1375 ± 44	0.068 ± 0.007	0.024 ± 0.003	0.896
10–15%	1170 ± 26	0.048 ± 0.005	0.015 ± 0.002	0.850
20–30%	702 ± 24	0.055 ± 0.007	0.017 ± 0.003	0.566
30–40%	502 ± 15	0.039 ± 0.006	0.010 ± 0.003	0.817
40–50%	309 ± 14	0.038 ± 0.008	0.012 ± 0.003	0.805
50–60%	181 ± 4	0.030 ± 0.004	0.010 ± 0.002	1.159
60–70%	96 ± 2	0.022 ± 0.004	0.010 ± 0.003	0.881
70–80%	44 ± 1	0.022 ± 0.006	0.018 ± 0.005	1.623
80–91%	23 ± 1	0.017 ± 0.004	0.010 ± 0.002	1.753

Table 6. Parameter values for charged kaons (averaged) produced in AuAu collision at $\sqrt{s_{NN}} = 130$ GeV.

Centrality	C_3	α (c/GeV)	β $(c/\mathrm{GeV})^2$	χ^2/n.d.f.
0–5%	175 ± 38	0.049 ± 0.009	0.018 ± 0.007	0.276
5–15%	135 ± 6	0.052 ± 0.009	0.017 ± 0.007	0.489
15–30%	79 ± 3	0.047 ± 0.008	0.016 ± 0.008	0.440
30–60%	32 ± 4	0.029 ± 0.006	0.014 ± 0.005	0.150
60–90%	4.2 ± 0.5	0.019 ± 0.008	0.012 ± 0.001	0.322

Table 7. Parameter values for charged kaons (averaged) produced in AuAu collision at $\sqrt{s_{NN}} = 200$ GeV.

Centrality	C_3	α (c/GeV)	β $(c/\mathrm{GeV})^2$	χ^2/n.d.f.
0–5%	150 ± 10	0.081 ± 0.010	0.034 ± 0.006	0.622
10–15%	115 ± 7	0.080 ± 0.011	0.033 ± 0.006	1.163
20–30%	70 ± 9	0.076 ± 0.009	0.031 ± 0.005	1.067
30–40%	45 ± 8	0.070 ± 0.009	0.026 ± 0.006	0.659
40–50%	30 ± 7	0.060 ± 0.008	0.026 ± 0.005	0.806
50–60%	15 ± 5	0.054 ± 0.007	0.024 ± 0.005	1.441
60–70%	7 ± 1	0.043 ± 0.007	0.022 ± 0.004	0.996
70–80%	3.0 ± 0.4	0.034 ± 0.005	0.021 ± 0.004	1.762
80–91%	1.4 ± 0.1	0.025 ± 0.004	0.020 ± 0.003	2.015

Table 8. Parameter values for the production of secondary protons in AuAu collision at $\sqrt{s_{NN}} = 130$ GeV.

Centrality	C_3	α (c/GeV)	β $(c/\mathrm{GeV})^2$	χ^2/n.d.f.
0–5%	23 ± 5	0.21 ± 0.03	0.045 ± 0.011	1.028
5–15%	16 ± 3	0.22 ± 0.02	0.053 ± 0.008	0.895
15–30%	12 ± 2	0.19 ± 0.02	0.042 ± 0.008	0.936
30–60%	6.0 ± 0.3	0.15 ± 0.01	0.031 ± 0.003	0.953
60–90%	1.0 ± 0.1	0.011 ± 0.02	0.023 ± 0.006	2.023

Table 9. Parameter values for the production of secondary protons in AuAu collision at $\sqrt{s_{NN}} = 200$ GeV.

Centrality	C_3	α (c/GeV)	β $(c/\mathrm{GeV})^2$	χ^2/n.d.f.
0–5%	19 ± 3	0.19 ± 0.02	0.037 ± 0.004	1.526
10–15%	17 ± 4	0.18 ± 0.02	0.034 ± 0.005	0.927
20–30%	12 ± 2	0.16 ± 0.02	0.030 ± 0.004	1.085
30–40%	8 ± 1	0.15 ± 0.01	0.027 ± 0.003	1.001
40–50%	6.5 ± 0.7	0.13 ± 0.02	0.025 ± 0.005	1.703
50–60%	4.0 ± 0.5	0.12 ± 0.01	0.023 ± 0.003	1.494
60–70%	1.9 ± 0.3	0.11 ± 0.01	0.020 ± 0.004	1.896
70–80%	0.8 ± 0.1	0.10 ± 0.01	0.017 ± 0.003	2.116
80–91%	0.50 ± 0.05	0.08 ± 0.01	0.015 ± 0.002	1.839

Table 10. Parameter values for the production of secondary antiprotons in AuAu collision at $\sqrt{s_{NN}} = 130$ GeV.

Centrality	C_3	α (c/GeV)	β $(c/\text{GeV})^2$	χ^2/n.d.f.
0–5%	13 ± 2	0.27 ± 0.02	0.050 ± 0.008	1.336
5–15%	8 ± 2	0.28 ± 0.03	0.052 ± 0.010	1.652
15–30%	7.3 ± 0.5	0.24 ± 0.01	0.049 ± 0.005	1.215
30–60%	3.7 ± 0.5	0.22 ± 0.01	0.046 ± 0.007	1.658
60–90%	0.5 ± 0.1	0.18 ± 0.02	0.028 ± 0.011	1.958

Table 11. Parameter values for the production of secondary antiprotons in AuAu collision at $\sqrt{s_{NN}} = 200$ GeV.

Centrality	C_3	α (c/GeV)	β $(c/\text{GeV})^2$	χ^2/n.d.f.
0–5%	8.6 ± 0.7	0.27 ± 0.02	0.048 ± 0.003	1.173
10–15%	8.5 ± 0.8	0.26 ± 0.01	0.046 ± 0.002	1.102
20–30%	5.8 ± 0.7	0.25 ± 0.01	0.043 ± 0.003	1.436
30–40%	4.1 ± 0.6	0.23 ± 0.01	0.042 ± 0.004	1.269
40–50%	3.0 ± 0.3	0.22 ± 0.01	0.040 ± 0.003	1.126
50–60%	2.2 ± 0.3	0.20 ± 0.01	0.039 ± 0.004	1.059
60–70%	1.5 ± 0.1	0.17 ± 0.02	0.034 ± 0.003	1.481
70–80%	0.6 ± 0.1	0.15 ± 0.01	0.033 ± 0.005	1.470
80–91%	0.32 ± 0.05	0.14 ± 0.01	0.029 ± 0.006	1.994

Table 12. Values of different parameters to obtain the "Fit" for α on the basis of eq. (9).

Secondary type	Collision energy	R (c/GeV)	S (c/GeV)
$\frac{h^+ + h^-}{2}$	130 GeV	0.036	0.0085
	200 GeV	0.018	0.0085
$\frac{\pi^+ + \pi^-}{2}$	130 GeV	0.023	0.0085
	200 GeV	0.0003	0.0087
$\frac{K^+ + K^-}{2}$	130 GeV	-0.011	0.011
	200 GeV	0.001	0.015
P	130 GeV	0.052	0.026
	200 GeV	0.034	0.027
$\bar{P}$	130 GeV	0.11	0.025
	200 GeV	0.010	0.026

Table 13. Values of different parameters to obtain the "Fit" for β on the basis of eq. (9).

Secondary type	Collision energy	R $(c/\text{GeV})^2$	S $(c/\text{GeV})^2$
$\frac{h^+ + h^-}{2}$	130 GeV	0.0035	0.0021
	200 GeV	0.0001	0.0019
$\frac{\pi^+ + \pi^-}{2}$	130 GeV	0.008	0.0019
	200 GeV	0.0055	0.0019
$\frac{K^+ + K^-}{2}$	130 GeV	0.006	0.0019
	200 GeV	0.016	0.0020
P	130 GeV	0.012	0.005
	200 GeV	0.0039	0.0048
$\bar{P}$	130 GeV	0.022	0.0051
	200 GeV	0.020	0.0048

manner with the help of eq. (9). The GCM-based results on $\langle p_{\text{T}} \rangle$ values are plotted in fig. 7. The different centrality values, the particle species and the interaction energy values are separately mentioned in each of the diagrams.

4 Concluding remarks

The chosen model appears to present essentially a universal approach in the sense that i) it provides a unified description of data on particle production in nuclear collisions in terms of the basic PP interaction; ii) the method could be applied in an integrated and uniform way without introduction of any artificial divide between the so-called "soft" (low-p_{T}) and "hard" (large-p_{T}) interactions; iii) the general approach remains valid, irrespective of whether the collisions are central or peripheral; iv) it has no model- or mechanism-specific physical picture as the input and as the constraint as well; v) the values of α and β, which are the only arbitrary parameters, need to be assumed and they demand tuning and adjustment on a case-to-case basis in an interaction-specific, secondary-specific and centrality-specific manner. So, the model seems to provide a universal, useful and economical description of a large body of data on high-energy heavy-ion collisions. The model is useful, as it is seen to give a fair account of the vast amount of data; and it is economical, because there are only two arbitrary parameters along with one normalization term for the general studies on heavy-ion reactions at high energies.

The agreements between the measured and/or extracted data and the phenomenological outputs are quite satisfactory on an overall basis of the p_{T} spectra and the $\langle p_{\text{T}} \rangle$-*vs.*-centrality diagrams. The only exception is the case of the average-transverse-momenta values of kaons in AuAu reaction at $\sqrt{s_{NN}} = 200$ GeV. Though we cannot readily ascribe any reason for such departure, there is a

general observation that the measurements related to any variety of the strange particles suffer, in general, a higher degree of uncertainty. Besides, we also fail to explain here how and why this phenomenological approach works functionally so well. No clue to any concrete physical reason arising out of some underlying dynamics of particle and nuclear interactions could be immediately ascertained. The harmony revealed in the natures of α and β *vs.* various $N_{\rm part}$ values reflecting various centrality of the reactions is certainly an interesting observation from the present approach. The closeness of the values of S in the table 12 and table 13 at two different neighbourly energies appears to indicate the fact that, beyond a certain value of $N_{\rm part}$, the enhancement of the centrality of the collision with the increase in the number of wounded nucleons, *i.e.* $N_{\rm part}$ does not necessarily and appreciably raise the values of $\langle p_{\rm T} \rangle$ for any variety of the secondaries. This brings out strong hints to what is called parton saturation at and after a definite value of $N_{\rm part}$. *In fine*, in so far as the actual performance is concerned, the model has a modest degree of success. However, one major drawback in applying this approach is it's over-reliance on the availability of the measured and dependable data sets on the specific variety of the secondary in the PP interaction at some definite energies and at certain reasonable intervals in the energy values in order to construct the energy-dependence profile for some parameters to be used in the model. Secondly, the final working formula for studying the properties of nuclear collisions in the present work does neither contain directly, nor exhibit any of the technicalities of the nuclear geometry, *e.g.*, the impact parameter (denoted generally by b) or of the space-time evolution scenarios of the nuclear collisions. The entirety of the nuclear effects is taken care of by the simple product term $(AB)^{f(y,p_{\rm T})}$. This simplicity of form could very well be viewed in a positive way in favour of the model.

The authors would like to express their thankful gratitude to the anonymous referee for his/her critical remarks and valuable suggestions for the improvement of an earlier draft of the manuscript.

References

1. PHENIX Collaboration (T. Chujo), talk presented at *Quark Matter 2002, Proceedings of the 16th International Conference on Ultra-Relativistic Nucleus-Nucleus Collisions, Nantes, France, 18-24 July 2002*, edited by H. Gutbrod, J. Aichelin, K. Werner, Nucl. Phys. A **715**, 151 (2003) and references therein, nucl-ex/0209027, `http://www.phenix.bnl.gov/WWW/publish/chujo/presentation/QM2002_chujo_v2.pdf`.
2. PHENIX Collaboration (S. Mioduszewski), talk presented at *Quark Matter 2002, Proceedings of the 16th International Conference on Ultra-Relativistic Nucleus-Nucleus Collisions, Nantes, France, 18-24 July 2002*, edited by H. Gutbrod, J. Aichelin, K. Werner, Nucl. Phys. A **715**, 199 (2003), nucl-ex/0210021.
3. PHENIX Collaboration (J. Jia), talk presented at *Quark Matter 2002, Proceedings of the 16th International Conference on Ultra-Relativistic Nucleus-Nucleus Collisions, Nantes, France, 18-24 July 2002*, edited by H. Gutbrod, J. Aichelin, K. Werner, Nucl. Phys. A **715**, 769 (2003), nucl-ex/0209029, `http://www.phenix.bnl.gov/WWW/publish/jjia/qm02.pdf`.
4. STAR Collaboration (C. Adler *et al.*), Phys. Rev. Lett. **89**, 202301 (2002).
5. PHENIX Collaboration (J.M.B. Hoy), PhD Thesis, State University of New York at Stony Brook (`http://www.phenix.bnl.gov/thesis.html`).
6. M.A. Faessler, Phys. Rep. **115**, 1 (1984).
7. T. Peitzmann, Phys. Lett. B **450**, 7 (1999).
8. H.R. Schmidt, J. Schukraft, J. Phys. G **19**, 1705 (1993).
9. R. Hagedorn, Riv. Nuovo Cimento **6**, 1 (1983).
10. WA98 Collaboration (M.M. Aggarwal *et al.*), Eur. Phys. J. C **23**, 225 (2002).
11. WA80 Collaboration (R. Albrecht *et al.*), Eur. Phys. J. C **5**, 255 (1998).
12. D. Antreasyan *et al.*, Phys. Rev. D **19**, 764 (1979).
13. S. Bhattacharyya, Lett. Nuovo Cimento **44**, 119 (1985).
14. Bhaskar De, S. Bhattacharyya, P. Guptaroy, J. Phys. G **28**, 2963 (2002).
15. Bhaskar De, S. Bhattacharyya, to be published in Int. J. Mod. Phys. A, hep-ph/0306089.
16. Bhaskar De, S. Bhattacharyya, P. Guptaroy, Eur. Phys. J. A **16**, 415 (2003).
17. Bhaskar De, S. Bhattacharyya, Mod. Phys. Lett. A **18**, 1383 (2003), nucl-th/0211031.
18. R.C. Hwa, C.B. Yang, Phys. Rev. C **67**, 034902 (2003).